Calculation of the renal perfusion and glomerular filtration rate from the renal impulse response obtained with MRI

L. Hermoye[1], L. Annet[1], Ph. Lemmerling[2], F. Peeters[1], F. Jamar[3], P. Gianello[4], S. Van Huffel[2], B.E. Van Beers[1]

[1]Department of Radiology and Center for Anatomical, Functional and Molecular Imaging Research, Université Catholique de Louvain, St-Luc University Hospital, Brussels, Belgium

[2]Department of Electrical Engineering, Katholieke Universiteit Leuven, Leuven, Belgium

[3] Division of Nuclear Medicine and Center for Anatomical, Functional and Molecular Imaging Research, Université Catholique de Louvain, St-Luc University Hospital, Brussels, Belgium

[4] Laboratory of Experimental Surgery, Université Catholique de Louvain, Brussels, Belgium

Corresponding author: Laurent Hermoye
Department of Radiology
Université Catholique de Louvain
St-Luc University Hospital
Avenue Hippocrate 10
B-1200 Brussels, Belgium
Tel: 32-2-7642787
Fax: 32-2-7649076
Email: hermoye@rdgn.ucl.ac.be

Grant sponsors: Fonds National de la Recherche Scientifique, Research Council of the Katholieke Universiteit Leuven , Program on Interuniversity Poles of Attraction, Flemish Community, and Fonds voor Wetenschappelijk Onderzoek, Belgium. Grant numbers: FRSM 3.4578.00, IDO/99/03, IDO/02/009, IUAP Phase V-22, MEFISTO-666, G.0078.01, G.0269.02 and G.0270.02. Laurent Hermoye is a PhD student funded by the Fonds Special de Recherche. Philippe Lemmerling is a Postdoctoral Fellow of the Fonds voor Wetenschappelijk Onderzoek.

Running head: In vivo renal perfusion and GFR measurement

Word count: 6977

Abstract

The aim of this study was to assess the importance of deconvolution for the calculation of renal perfusion and glomerular filtration rate (GFR) on the basis of concentration-time curves as measured with perfusion MRI. Six rabbits were scanned dynamically after injection of a gadolinium chelate. Concentration-time curves were generated by manually drawing regions of interest in the aorta and the renal cortex. To remove the dependency on the arterial input function, a regularized structured total least squares deconvolution algorithm was used to calculate the renal impulse response. This curve was fitted by the sum of two gamma variate functions, corresponding to the passage of the contrast agent in the glomeruli and the proximal convoluted tubules. Tracer kinetics models were applied to these two functions to obtain the renal perfusion and GFR. For comparison, these two parameters were also calculated on the basis of the renal concentration-time curve before deconvolution. The renal perfusion values correlated well ($r = 0.9$, $p = 0.014$) with the values calculated by a validated upslope method. The GFR values correlated well ($r = 0.9$, $p = 0.014$) with the values obtained from the clearance of ^{51}Cr-EDTA. A comparison of the values obtained with and without deconvolution demonstrated the necessity of deconvolution.

Key words: magnetic resonance imaging, kidney, perfusion, glomerular filtration, deconvolution, contrast media.

Introduction

Renal perfusion and glomerular filtration rate (GFR) are important parameters in the diagnosis of several renal diseases, including renal failure, renal artery stenosis, and renal graft rejection. Various methods have been used to measure renal perfusion and GFR but these methods have important limitations. The reference method to measure renal blood flow is to place a flowmeter around the renal artery or to inject radiolabeled microspheres into the renal artery. Unfortunately, these methods are invasive. The gold standard for the measurement of GFR is the renal clearance of inulin. However, this method is cumbersome and not practical for routine clinical use because of the difficulty of obtaining complete, accurately timed urine collections. The clearance of creatinine, an endogenous substance, can be used instead of the clearance of inulin but the need for timed urine collection remains. In clinical practice, plasma creatinine is often used as a marker of glomerular function. However, because of tubular secretion and extrarenal excretion of creatinine and variations depending on muscular mass, plasma creatinine is a very poor index of the GFR when modest reductions in that rate occur (1).

Radionuclides can be used to measure both renal blood flow and GFR (2). Substances that are cleared by glomerular filtration and tubular secretion yield renal blood flow; substances that are rapidly and totally cleared by glomerular filtration give a measurement of GFR. Of the various radiopharmaceuticals available, ^{99m}Tc-DTPA and ^{51}Cr-EDTA are used for the estimation of GFR whereas ^{123}I-Hippuran is used for renal perfusion. These methods require the injection of radioactive material and several blood samples need to be taken.

All the methods based on plasma clearance measure the total renal blood flow and GFR. The separate measurement of these parameters for the two kidneys would improve the diagnosis of various renal diseases. Imaging methods can be used for this purpose. A renogram can be generated by following the activity of a radionuclide in the two kidneys with a gamma camera. Background correction is necessary and cumbersome, hampering accurate quantitative

measurements of GFR using gamma camera techniques. Doppler ultrasound can only measure renal blood flow. Furthermore, in a certain percentage of patients, the examinations are inadequate because of obesity or presence of bowel gas (3).

In contrast, perfusion MRI and computed tomography (CT) make it possible to obtain images with high temporal and spatial resolution. Phase contrast imaging can be used to measure renal blood flow (4). This method cannot be used to measure the GFR and requires drawing a region of interest in the renal artery. Since this artery is small, the region of interest only comprises a few pixels and is therefore very sensitive to noise. Krier et al. (5) proposed to fit the renal cortical concentration-time curve by a sum of three gamma variate functions, representing the passage of the contrast agent in the glomeruli, the proximal convoluted tubules, and the distal convoluted tubules. They calculated the renal perfusion and GFR on the basis of the area, mean transit time and maximum of these three functions. If the shape of the arterial input function is not taken into account, important errors can arise with their method because of the dispersion and the recirculation of the contrast agent. The aim of this study is to evaluate the influence of these two effects on the calculated renal perfusion and GFR. To remove the dependency on the arterial input function, we calculated the renal perfusion and GFR on the basis of the renal impulse response obtained by deconvolution of the cortical concentration versus time curve by the arterial input function. The noise sensitivity of the method was assessed with computer simulations.

Methods

Experimental animal procedure

Experiments were performed on 6 male New Zealand White rabbits (Iffa Credo, Brussels, Belgium) with normal renal function. The age of the rabbits was 29 ± 17 weeks, their weight 3.1 ± 1.1 kg. The study protocol was approved by the ethics committee on animal care of our institution. The rabbits were housed in individual cages at 19°C with a 12-hour light-dark schedule.

Q1

The animals were anaesthetized with intramuscular injection of 25 mg/kg ketamine and 10 mg/kg xylazine. A 24-gauge catheter was inserted into the central ear vein for ^{51}Cr-EDTA injection (Bristol Myers Squibb, Brussels, Belgium, 20-40 µCi in 1 mL) and blood sampling. The animals were allowed to wake up after ^{51}Cr-EDTA injection. Three blood samples (2 mL) were taken 2, 3, and 4 hours after the injection. Two hours after the last blood sampling, the animals were anaesthetized again. The MR studies were performed 30 minutes after the start of the anaesthesia.

MR imaging technique

The studies were performed on a 1.5 T whole body MR scanner (Gyroscan NT Intera T15; Philips Medical Systems, Best, The Netherlands). A transverse slice at the level of the right kidney and the abdominal aorta was scanned dynamically after intravenous injection of 0.05 mmol/kg gadoterate dimeglumine (Dotarem; Guerbet, Roissy, France). The contrast material was manually injected at the beginning of the MR data acquisition through the catheter placed in the central ear vein, and flushed by 5 mL of saline solution. All bolus injections were performed by one investigator. 120 images were obtained using a non-triggered T1-weighted turbo field echo sequence with a non slice-selective saturation prepulse. Imaging parameters were: slice thickness = 4mm, field of view = 220*132mm, acquisition matrix = 256*76, flip angle = 15°, TE = 1.32 ms,

TR = 6.80 ms, single shot, number of excitations = 2, and acquisition time of 1132 ms per dynamic.

A 16-slice T1-weighted gradient echo sequence (slice thickness = 4 mm, slice gap = 0.4 mm, field of view = 260*156 mm, acquisition matrix = 512*308, flip angle = 80°, TE = 1.72 ms, TR = 94 ms, number of excitations = 1) was also acquired to measure the volume of the kidneys.

Signal conversion

Data processing was performed on a HP X4000 workstation (Hewlett-Packard, Palo Alto, CA), using homemade programs written in IDL 5.4 (Research Systems Inc., Boulder, CO) and Matlab 5.3 (Mathworks, Natick, MA). Signal intensity versus time curves were obtained by manually drawing regions of interest in the aorta (mean area = 16 mm^2) and the renal cortex (mean area = 180 mm^2) (Figure 1). These curves were converted into concentration versus time curves in two steps as previously described (6). In the first step, the signal intensity was converted into longitudinal relaxation rate (R_1) by using a calibration curve obtained from a phantom consisting of tubes filled with different concentrations of gadoterate dimeglumine. In the second step, a linear relationship was assumed between R_1 and contrast agent concentration (C), according to the equation:

$$R_1 = R_{10} + r.C \qquad [1]$$

where R_{10} is the longitudinal relaxation rate before contrast agent injection and r is the longitudinal relaxivity of the contrast agent. This relationship assumes a constant relaxivity in blood and tissue and fast transcytolemmal water exchange. The concentration in the aorta was divided by (1-hematocrit) to obtain the plasmatic concentration. The hematocrit was assumed equal to 0.45 for all the rabbits.

Deconvolution algorithm and curve fitting

The renal impulse response (IR) *h(t)* is defined as the concentration versus time curve that would have been measured in the renal cortex if the arterial input function was an unit impulse. The cortical concentration versus time curve ($C_{ROI}(t)$) can be written as the convolution of the arterial input function ($C_{AIF}(t)$) and the renal impulse response (7):

$$C_{ROI}(t) = C_{AIF}(t) \otimes h(t) , \qquad [2]$$

where $\otimes$ denotes the convolution operator.

The renal impulse response can therefore be obtained by performing the inverse operation:

$$h(t) = C_{ROI}(t) \otimes^{-1} C_{AIF}(t) . \qquad [3]$$

Mathematically, the latter operation comes down to solving a set of linear equations:

$$Ih \approx r \qquad [4]$$

where *I* is a Toeplitz matrix specified by its first column containing $C_{AIF}(t)$ and the fact that above the main diagonal, *I* only contains zeroes. Furthermore, *r* is a column vector, with $r(i) = C_{ROI}(i)$ and *h* represents the renal impulse response. It has been previously shown (8) that the statistical accuracy of the solution of the latter set of equations can be improved by using a so-called structured total least squares (STLS) approach. This approach simply forces the correction matrix applied to *I*, in order to obtain a set of consistent equations, to have the same structure as the matrix *I* itself. However, since the matrix *I* is ill-conditioned, small perturbations to the data can yield large differences in the renal impulse response *h*. This effect is minimized by means of regularization, i.e. by using the regularized STLS approach (9). A regularized structured total least squares algorithm was used to perform the numerical deconvolution. The value of the regularization parameter was chosen such that the convolution of the arterial input function and renal impulse response did not show severe oscillations due to the inherent noise. Because of the linearity of the deconvolution operation, and if the longitudinal relaxivity is assumed constant in blood and tissue, this operation can be performed on the longitudinal relaxation rate (R_1-R_{10}) versus time curves. This removes the need to measure the exact value of the relaxivity. To assess the quality of the deconvolution, the curve obtained by convolution of the

arterial input function and the renal impulse response was compared with the cortical concentration versus time curve.

It is expected that the renal impulse response exhibits three sequential peaks corresponding to the passage of the contrast agent in the glomeruli, the proximal convoluted tubules, and the distal convoluted tubules (10). The Levenberg-Marquardt non-linear least squares fitting algorithm was used to fit the first two peaks by a sum (*G(t)*) of two gamma variate functions, according to the equation:

$$G(t) = a_1 (t - a_4)^{a_2} e^{\frac{-(t-a_4)}{a_3}} + b_1 (t - b_4)^{b_2} e^{\frac{-(t-b_4)}{b_3}} \qquad [5]$$

where t is the time and the a_i and b_i are the parameters to fit. The quality of the fit was measured as the mean squared distance between the real impulse response and the sum of the two gamma functions. For comparison, the first two peaks of the cortical concentration versus time curve without deconvolution were fitted by a sum of two gamma variate functions using the same algorithm.

Calculation of renal perfusion, GFR, and filtration fraction

According to the central volume theorem (11), the renal plasmatic perfusion was calculated as the ratio of the fractional plasma volume (FPV) by the vascular mean transit time (MTT):

$$\text{Renal perfusion} = \frac{\text{FPV}}{\text{Vascular MTT}} \qquad [6]$$

where the renal perfusion is expressed in mL min^{-1} mL^{-1}. The FPV is usually determined as the ratio of the areas under the tissue curve and the arterial input function. However, as the input function of the renal impulse response is a unit impulse (area = 1), the FPV equals the area under the vascular peak of the renal impulse response (12). The vascular MTT was calculated as the centroid (i.e. normalized first moment) of the vascular outflow curve (13), which was obtained by temporal derivation of the vascular peak of the renal impulse response. The results obtained with this method were correlated with those of a maximum upslope method as described and validated

by Peters et al. (14). Moreover, for comparison, the renal perfusion was calculated on the renal concentration versus time curve without deconvolution using the same formula (Eq. [6]). The FPV was calculated as the ratio of the areas under the vascular peak of the cortical concentration versus time curve and the arterial input function. To exclude the recirculation, a gamma variate function was fitted on the arterial input function. The vascular MTT was obtained as the first moment of the temporal derivative of the vascular peak.

To calculate the GFR, an upslope method was used. The GFR (mL min^{-1} mL^{-1}) was calculated according to the following equation:

$$GFR = \frac{\text{maximum slope of the proximal tubule peak}}{(C_{vasc})_{max}}. \qquad [7]$$

To calculate $(C_{vasc})_{max}$, the maximum of the vascular peak was divided by the FPV to take into account that the contrast medium remains extracellular. The total GFR (mL min^{-1}) was obtained by multiplying the GFR expressed per mL of tissue by the volume of the renal cortex. The volume of the renal cortex was assumed to equal 70 % of the total kidney volume (15). The results of GFR were correlated with those obtained by the clearance of ^{51}Cr-EDTA. Again, for comparison, the GFR was calculated directly on the renal concentration versus time curve without deconvolution using the same formula. The filtration fraction (FF in %) was calculated as the ratio of the GFR and the renal perfusion (RP), both expressed per mL of tissue:

$$FF = \frac{GFR}{RP}. \qquad [8]$$

GFR measurement with ^{51}Cr-EDTA

The exact activity per unit volume of ^{51}Cr-EDTA was measured by counting the activity of a diluted aliquot in a gamma counter (Cobra II, Auto-Gamma Packard, Downers Grove, IL). The exact injected volume was measured by weighing the syringe before and after injection (density equal to 1.0 was assumed). Three blood samples (1 - 2 mL) were taken in each rabbit 2, 3, and 4 hours after the injection. The samples were centrifuged to obtain plasma samples (0.5 - 1mL). The

activity of these samples was counted in the gamma counter. The distribution volume and the radioactive constant of the agent were calculated on the basis of these three measurements. The GFR was calculated as the product of the distribution volume and the radioactive constant, as described by Chantler et al. (16). The correction factor proposed by Chantler et al. was used. This factor corrects for tubular reabsorption, venous sampling, and biexponential decay (16).

Computer simulations

To analyze the sensitivity to noise of the method, computer simulations were performed using the Matlab (Mathworks, Natick, MA) and IDL (Research Systems Inc., Boulder, CO) programming languages. An ideal arterial input function was generated by smoothing a real one. An ideal renal impulse response was created by summing two gamma variate functions. The ideal tissue curve was obtained as the convolution of the ideal arterial input function with the ideal impulse response, according to Eq. [2]. The ideal perfusion, GFR, and filtration fraction were calculated on the basis of the ideal renal impulse response. To analyze the sensitivity to noise of these parameters, gaussian noise was added to the tissue curve and the arterial input function. The standard deviation of the noise was expressed as a percentage (from 0% to 10%) of the peak of each curve. For each percentage, the renal impulse response was calculated as the deconvolution of the noised tissue curve with the noised arterial input function. The regularization parameter was automatically adjusted to minimize the squared distance between the ideal and reconstructed curves. For each percentage, the reconstructed impulse response was fitted by the sum of two gamma variate functions. The renal perfusion, GFR, and filtration fraction were calculated on the basis of the fitted functions. For each measurement, the relative error was obtained by dividing the distance between the calculated and ideal values by the ideal value. The regularization parameter and the squared distance between the ideal and reconstructed curves were also recorded.

To calculate the noise percentage encountered in the real curves, the end of the arterial input function and the tissue curve were assumed linear. A linear regression was performed on this part

for each curve. The residuals of the regression then represent the noise. The standard deviation of the residuals was divided by the peak of each curve to obtain the noise percentage.

Statistical analysis

Numerical values are expressed as mean ± standard deviation. The statistical analysis was performed with the SPSS software (SPSS Inc., Chicago, IL). Correlations were assessed with Pearson correlation coefficients. A *p*-value less than .05 was considered statistically significant.

Results

Perfusion and GFR measurements

As expected, the renal impulse response exhibited three sequential peaks in the six rabbits (Figure 2). Multiple proximal tubular peaks were found in two rabbits. Before deconvolution, three of the six cortical concentration versus time curves did not exhibit sequential peaks (Figure 3). A sum of two gamma variate functions could be fitted on the six renal impulse responses (Figure 2) (mean squared distance = $2.5*10^{-6}$), but only on three concentration versus time curves before deconvolution (Figure 4). A good correspondence (mean squared distance = $2.5*10^{-3}$) was found between the measured tissue curve and the reconstructed tissue curve obtained by convolution of the arterial input function and the renal impulse response . The mean fractional plasma volume was 15 ± 5 % (averaged over all six rabbits). The mean vascular MTT was 6.8 ± 1.7 s. A mean renal perfusion of 1.3 ± 0.4 mL min^{-1} mL^{-1} was obtained. A significant correlation (r = 0.9, p = 0.014) (Figure 5a) was found between the renal perfusion values found with this method and the maximum upslope method. The equation of the regression line is Y = 1.12 X – 0.24, where Y are the values measured with the upslope method and X with the deconvolution method.

The mean GFR was 0.23 ± 0.07 mL min^{-1} mL^{-1}, the mean renal cortex size, 8.6 ± 1.0 mL, and the mean total GFR, 2.9 ± 1.0 mL min^{-1}. The results correlated well (r = 0.9, p = 0.014) (Figure 5b) with the values found with ^{51}Cr-EDTA but were smaller. The mean filtration fraction was 19 ± 7%.

For the comparison with the method without deconvolution, only the three rabbits showing sequential peaks on their cortical concentration versus time curve before deconvolution could be used. Without deconvolution, the following mean values (averaged over three rabbits) were obtained: fractional plasma volume 4 ± 2 %, vascular MTT 10.2 ± 1.4 s, renal perfusion 0.26 ± 0.18 mL min^{-1} mL^{-1}, GFR 3.8 ± 2.3 mL min^{-1}, and filtration fraction 183 ± 40 %. These results are of course unrealistic and will be discussed below.

Computer simulations

The ideal perfusion and GFR were 1.13 mL min^{-1} mL^{-1} and 0.26 mL min^{-1} mL^{-1}. The evolution of the relative error on the perfusion and GFR measurements is shown in figure 6a. When the added noise percentage varied from 0% to 10%, the relative errors of the perfusion measurement rised from 0% to –51%. The underestimation on the perfusion was mainly explained by a rise in the estimated MTT values as shown in figure 6b. The relative errors of the GFR measurements varied around 0 but no specific trend was observed. As expected, the regularization parameters rised from 0 to 500 with the noise percentage. Despite this rise, the mean squared distance between the ideal and reconstructed curve rised from 0 to 2.38 10^{-4}. The actual noise percentages measured on the real arterial and cortical curves were typically between 1% and 4%. As shown in figure 6a, the maximum relative error at these noise levels was 24%.

Discussion

Our results show that to calculate renal perfusion and glomerular filtration after intravenous injection of a contrast agent, it is important to perform a deconvolution before fitting the renal curve by a sum of two gamma variate functions. As can be seen in figure 1c, the real arterial input function is far from a unit impulse when peripheral injection of the contrast agent is performed. The length of the injection and the travel of the contrast medium through the heart, the pulmonary and systemic circulation induce dispersion. Furthermore, as the contrast medium is not completely filtered in one pass, its recirculation can be observed for several hours after the injection. The mean plasma elimination half-life of gadoterate dimeglumine is 91 minutes (17). The deconvolution removes the dependence of the calculated parameters on the arterial input function. If one omits this step, differences in injection scheme (manual or automatic), speed (bolus or infusion) and pulmonary or systemic circulation time would yield different results. Even with identical injection methods, the arterial input function has been shown to have a high interindividual variability (18). Without deconvolution, the peak corresponding to the passage of the contrast medium in the proximal tubule is highly overestimated because of the recirculation (Figure 4). As a result the vascular peak is underestimated in the fit. The fractional plasma volume and the maximum concentration of the vascular peak are thus underestimated. The maximum slope of the proximal tubular peak is overestimated. The vascular MTT is overestimated because of the dispersion of the arterial input function. All these effects combined lead to a severe underestimation of the renal perfusion and overestimation of the GFR. It is thus not surprising to find a filtration fraction higher than 100%. The results obtained without deconvolution are unrealistic. Furthermore, as the cortical concentration versus time curve is the result of the convolution of the arterial input function and the renal impulse response, the peaks are not always clearly apparent (Figure 3). Therefore, the fit does not always converge, making calculation of renal perfusion and GFR impossible. To minimize the dispersion of the bolus reaching the

kidneys, Krier et al. (5) injected the contrast agent in the superior vena cava or the right cardiac atrium. Even with this central injection, dispersion occurs in the pulmonary circulation, the left heart, and the systemic circulation. Furthermore, recirculation is unavoidable. A deconvolution should thus be performed. The necessity of deconvolution has not been assessed in previous studies of renal function (5,19). The importance of deconvolution has, however, been recognized in brain studies (20). Recently, deconvolution has been used to calculate the renal vascular impulse response (21,22). As an intravascular tracer was used in these renal studies, the GFR could not be calculated.

After deconvolution, we observed an excellent correlation between the measurements of renal perfusion and GFR and the measurements obtained by reference methods. However, the equation of the regression line for perfusion measurements did not exactly match the identity equation (Y = X). The hypotheses that underlie the two methods of perfusion measurement can explain the observed differences. The deconvolution method makes the assumption that the renal impulse response can be modelled by a sum of two gamma variate functions. This may be a simplification as the cortex contains superficial and juxtamedullary nephrons with different physiological parameters. The maximum upslope method makes the assumption that the tracer does not leave the renal glomeruli during the first upslope of the cortical curve. Our results show that tracer is already filtered at this stage. The assumptions may thus not be perfectly borne out by the facts. In addition, some scatter around the regression line can be expected because of experimental uncertainty, as shown by the results of the computer simulations.

A renal plasmatic perfusion of 1.3 ± 0.4 mL min^{-1} mL^{-1} is in agreement with the mean renal plasmatic perfusion of 1.4 mL min^{-1} mL^{-1} found in patients in other MRI studies (23). The renal perfusion has been shown to be independent of the species (24). The GFR values found with ^{51}Cr-EDTA are in the range of those found in other rabbit studies (25,26). The filtration fraction of 19 ± 7 % is in the normal range (27).

Q2

However, several effects can disturb the measurements and may explain the observed differences in GFR between MRI and ^{51}Cr-EDTA clearance. Use of Eq. [1] to determine the contrast agent concentration requires that the system be in the fast exchange limit (28,29). If not, biexponential longitudinal relaxation can result. The exchange regimen in the kidney remains debated. The exchange between the intra- and extracellular space should be intermediate to fast in the kidney as in other organs (30) and no significant errors in the calculation of the functional parameters should be expected, when using normal doses of contrast agents (31). However, the spin exchange may be slow during the tubular passage of the filtered bolus because of the compartmentalization of the contrast agent in the tubules and because the transport of water from the tubules to the renal interstitium is regulated (30,32). This slow exchange may decrease the signal intensity of the kidney, especially at later time points. Katzberg et al. observed that the signal intensity of gadolinium in vivo in the kidney five minutes after injection was much lower than that for comparable gadolinium concentrations in a phantom model (32).

Another source of errors can be inflow effects. The flow related enhancement will lead to an overestimation of the concentration of the arterial input function (33). Fortunately, inflow related errors can be corrected on the basis of time resolved flow measurements if the perfusion measurements are synchronized to the cardiac cycle (34). In this study, a non-triggered perfusion sequence was used because of the fast heart rate of the rabbits and this correction could not be used.

Our method assumes that the renal arterial input function can be approximated by the concentration versus time curve in the aorta. However, time delay and dispersion occur between the aorta and the glomeruli. These phenomena have been shown to result in a systematic underestimation of the parameters calculated with perfusion imaging (35,36). To solve this problem, the arterial input function should be measured directly in the renal artery. However, this artery is very small and the measurement is not always feasible. Another way to solve this problem is to mathematically delay and disperse the aortic curve (37). With this method, the delay

and dispersion are two additional parameters in the fit. In total, ten parameters should thus be fitted. This high number of parameters would lead to ill-conditioned problems.

Anaesthesia can also partly explain the underestimation of GFR with MRI relative to the clearance of ^{51}Cr-EDTA. Indeed, to avoid prolonged anaesthesia, the rabbits were awake during the blood collections performed for the measurements of ^{51}Cr-EDTA clearance, but were anaesthetized for MRI. As the ketamine-xylazine combination used for anaesthesia produces a 30 % decrease (from 100 mmHg to 70 mmHg) in mean blood pressure (38), the blood pressure conditions were thus different during the measurements of ^{51}Cr-EDTA clearance and MRI. With small drops of blood pressure, autoregulation mechanisms maintain renal perfusion and GFR at constant levels. However, at a mean blood pressure of 70 mmHg, the renal perfusion and GFR have been reported to drop to about 60% of their normal values in the rat (24). In addition, the GFR measured by the clearance of ^{51}Cr-EDTA is slightly overestimated because of some extrarenal clearance of the marker (39).

The multiple proximal tubular peaks found in two rabbits can be explained by the fact that the data matrix involved in the deconvolution problem is ill-conditioned, i.e. small perturbations in the data can yield large differences in the renal impulse response. This effect is minimized by means of regularization but cannot be completely removed. In addition, as already discussed, the nephrons found in the region of interest are heterogeneous (about 85% cortical nephrons and 15% juxtamedullary nephrons) and the contrast medium does not traverse all of them at the same time.

The noise levels obtained with the MRI perfusion sequence was 1 – 4%. These values are explained by the relatively low signal to noise ratio (SNR) of the perfusion images. Higher SNR can be obtained with longer acquisition times. However, errors might arise because of undersampling of the first bolus passage. In future studies, the use of higher field strengths (3 Tesla) might improve the SNR without compromising the temporal resolution. Breathing related motion also increased the noise level of the curves. Although the regions of interest were manually checked on each image, the motion effect could not be totally removed. With these

levels, the relative error in the measurements of the functional parameters was below 24 %. Similar results were observed in a previous liver perfusion study (6). This rather high value is explained by the fact that the noise in the initial curves is amplified by the deconvolution process. Filtering would diminish the noise level but would distort the curves.

Most renal perfusion studies published so far were performed with computed tomography (5,40,41). Computed tomography offers a better temporal and spatial resolution than MRI. Furthermore, a linear relationship is observed between signal enhancement and concentration of the contrast agent, which removes the need for complex signal calibration. Inflow effects and the rate of water exchange do not perturb the measurements at computed tomography. However, the use of iodinated contrast media can impair the renal function, especially in patients with pre-existing renal insufficiency (42). In addition, high radiation doses are administered when the same slice level is repeatedly scanned to build the signal intensity versus time curve. Therefore, MRI may be better suited than computed tomography for measuring functional parameters in the kidneys, especially in patients with poor renal function.

In conclusion, functional parameters calculated with contrast-enhanced MRI on the basis of the renal impulse response correlated well with those obtained with a reference method. Without deconvolution, unrealistic results were obtained.

Reference List

1. Cameron JS, Greger R. Renal function and testing of function. In: Davison AM, Grunfeld JP, Kerr DN, Winearls CG, editors. Oxford: Oxford Medical Publications; 2003. p 40-70.
2. Russell CD, Dubovsky EV. Measurement of renal function with radionuclides. J Nucl Med 1989;30:2053-2057.
3. De Cobelli F, Venturini M, Vanzulli A, Sironi S, Salvioni M, Angeli E, Scifo P, Garancini MP, Quartagno R, Bianchi G, Del Maschio A. Renal arterial stenosis: prospective comparison of color Doppler US and breath-hold, three-dimensional, dynamic, gadolinium-enhanced MR angiography. Radiology 2000;214:373-380.
4. Coulam CH, Lee JH, Wedding KL, Spielman DM, Pelc NJ, Kee ST, Hill BB, Bouley DM, Derby GC, Myers BD, Sawyer-Glover AM, Sommer FG. Noninvasive measurement of extraction fraction and single-kidney glomerular filtration rate with MR imaging in swine with surgically created renal arterial stenoses. Radiology 2002;223:76-82.
5. Krier JD, Ritman EL, Bajzer Z, Romero JC, Lerman A, Lerman LO. Noninvasive measurement of concurrent single-kidney perfusion, glomerular filtration, and tubular function. Am J Physiol Renal Physiol 2001;281:F630-F638.
6. Materne R, Smith AM, Peeters F, Dehoux JP, Keyeux A, Horsmans Y, Van Beers BE. Assessment of hepatic perfusion parameters with dynamic MRI. Magn Reson Med 2002;47:135-142.
7. Ostergaard L, Weisskoff RM, Chesler DA, Gyldensted C, Rosen BR. High resolution measurement of cerebral blood flow using intravascular tracer bolus passages. Part I: Mathematical approach and statistical analysis. Magn Reson Med 1996;36:715-725.

8. Abatzoglou TJ, Mendel JM, Harada GA. The constrained total least squares technique and its applications to harmonic superresolution. IEEE Transactions on Signal Processing 1991;39:1070-1086.
9. Mastronardi N, Lemmerling P, Van Huffel S. Fast regularized structured total least squares algorithm for solving the basic deconvolution problem. Internal report ESAT-SISTA, KUL (Leuven, Belgium) 2002;02-162
10. Wolf GL, Hoop B, Cannillo JA, Rogowska JA, Halpern EF. Measurement of renal transit of gadopentetate dimeglumine with echo- planar MR imaging. J Magn Reson Imaging 1994;4:365-372.
11. Meier P, Zierler KL. On the theory of the indicator-dilution method for measurement of blood flow and volume. J Appl Physiol 1954;6:731-744.
12. Perkio J, Aronen HJ, Kangasmaki A, Liu Y, Karonen J, Savolainen S, Ostergaard L. Evaluation of four postprocessing methods for determination of cerebral blood volume and mean transit time by dynamic susceptibility contrast imaging. Magn Reson Med 2002;47:973-981.
13. Weisskoff RM, Chesler D, Boxerman JL, Rosen BR. Pitfalls in MR measurement of tissue blood flow with intravascular tracers: which mean transit time? Magn Reson Med 1993;29:553-558.
14. Peters AM, Brown J, Hartnell GG, Myers MJ, Haskell C, Lavender JP. Non-invasive measurement of renal blood flow with 99mTc DTPA: comparison with radiolabelled microspheres. Cardiovasc Res 1987;21:830-834.
15. Hegedus V, Faarup P. Cortical volume of the normal human kidney. Correlated angiographic and morphologic investigations. Acta Radiol Diagn (Stockh) 1972;12:481-496.

16. Chantler C, Garnett ES, Parsons V, Veall N. Glomerular filtration rate measurement in man by the single injection methods using 51Cr-EDTA. Clin Sci 1969;37:169-180.
17. Le Mignon MM, Chambon C, Warrington S, Davies R, Bonnemain B. Gd-DOTA. Pharmacokinetics and tolerability after intravenous injection into healthy volunteers. Invest Radiol 1990;25:933-937.
18. Port RE, Knopp MV, Brix G. Dynamic contrast-enhanced MRI using Gd-DTPA: interindividual variability of the arterial input function and consequences for the assessment of kinetics in tumors. Magn Reson Med 2001;45:1030-1038.
19. de Priester JA, den Boer JA, Christiaans MH, Kessels AG, Giele EL, Hasman A, van Hooff HP, van Engelshoven JM. Automated quantitative evaluation of diseased and nondiseased renal transplants with MR renography. J Magn Reson Imaging 2003;17:95-103.
20. Perthen JE, Calamante F, Gadian DG, Connelly A. Is quantification of bolus tracking MRI reliable without deconvolution? Magn Reson Med 2002;47:61-67.
21. Aumann S, Schoenberg SO, Just A, Briley-Saebo K, Bjornerud A, Bock M, Brix G. Quantification of renal perfusion using an intravascular contrast agent (part 1): Results in a canine model. Magn Reson Med 2003;49:276-287.
22. Schoenberg SO, Aumann S, Just A, Bock M, Knopp MV, Johansson LO, Ahlstrom H. Quantification of renal perfusion abnormalities using an intravascular contrast agent (part 2): Results in animals and humans with renal artery stenosis. Magn Reson Med 2003;49:288-298.
23. Vallee JP, Lazeyras F, Khan HG, Terrier F. Absolute renal blood flow quantification by dynamic MRI and Gd-DTPA. Eur Radiol 2000;10:1245-1252.
24. Dworkin LD, Sun AM, Brenner BM. The renal circulations. In: Brenner BM, editor. The kidney. Philadelphia: W.B. Saunders Company; 2000. p 277-318.

25. Tvedegaard E, Kamstrup O. Radioactive chromium-ethylenediaminetetraacetic acid for determination of glomerular filtration rate in rabbits. Lab Anim Sci 1981;31:688-692.

26. Prevot A, Semama DS, Justrabo E, Guignard JP, Escousse A, Gouyon JB. Acute cyclosporine A-induced nephrotoxicity: a rabbit model. Pediatr Nephrol 2000;14:370-375.

27. Tortora GJ, Grabowski SR. Principles of anatomy and physiology. New York: John Wiley & Sons; 2002. 1055 p.

28. Landis CS, Li X, Telang FW, Coderre JA, Micca PL, Rooney WD, Latour LL, Vetek G, Palyka I, Springer CS, Jr. Determination of the MRI contrast agent concentration time course in vivo following bolus injection: effect of equilibrium transcytolemmal water exchange. Magn Reson Med 2000;44:563-574.

29. Buckley DL. Transcytolemmal water exchange and its affect on the determination of contrast agent concentration in vivo. Magn Reson Med 2002;47:420-424.

30. den Boer JA, de Priester JA, van Engelshoven JM. Slow spin exchange explains the effects of diuresis on gadolinium enhancement in MR imaging in the kidney, not in other organs. Acad Radiol 2003;10:567-569.

31. Larsson HB, Rosenbaum S, Fritz-Hansen T. Quantification of the effect of water exchange in dynamic contrast MRI perfusion measurements in the brain and heart. Magn Reson Med 2001;46:272-281.

32. Katzberg RW, Ivanovic M, Buonocore MH, Pellot-Barakat C, Brock JM, Ryan JM, Whang K. Gadolinium-enhanced T1-weighted renal and abdominal MR imaging: quantitative discrepancy between clinical and in vitro findings. Acad Radiol 2002;9:679-687.

33. Montet X, Ivancevic MK, Belenger J, Jorge-Costa M, Pochon S, Pechere A, Terrier F, Vallee JP. Noninvasive measurement of absolute renal perfusion by contrast medium-enhanced magnetic resonance imaging. Invest Radiol 2003;38:584-592.
34. Peeters F, Annet L, Hermoye L, Van Beers BE. Inflow effect in TFE-imaging with application to perfusion measurements. Proceedings of the International Society for Magnetic Resonance in Medicine, Honolulu 2002
35. Schmitt M, Viallon M, Thelen M, Schreiber WG. Quantification of myocardial blood flow and blood flow reserve in the presence of arterial dispersion: a simulation study. Magn Reson Med 2002;47:787-793.
36. Calamante F, Gadian DG, Connelly A. Delay and dispersion effects in dynamic susceptibility contrast MRI: simulations using singular value decomposition. Magn Reson Med 2000;44:466-473.
37. Iida H, Higano S, Tomura N, Shishido F, Kanno I, Miura S, Murakami M, Takahashi K, Sasaki H, Uemura K. Evaluation of regional differences of tracer appearance time in cerebral tissues using [15O] water and dynamic positron emission tomography. J Cereb Blood Flow Metab 1988;8:285-288.
38. Sanford TD, Colby ED. Effect of xylazine and ketamine on blood pressure, heart rate and respiratory rate in rabbits. Lab Anim Sci 1980;30:519-523.
39. Frennby B, Sterner G, Almen T, Chai CM, Jonsson BA, Mansson S. Clearance of iohexol, chromium-51-ethylenediaminetetraacetic acid, and creatinine for determining the glomerular filtration rate in pigs with normal renal function: comparison of different clearance techniques. Acad Radiol 1996;3:651-659.
40. Tsushima Y, Blomley MJ, Kusano S, Endo K. Use of contrast-enhanced computed tomography to measure clearance per unit renal volume: a novel measurement of renal function and fractional vascular volume. Am J Kidney Dis 1999;33:754-760.

41. Itano NB, Sherrill LE, Lerman LO, Corica FA, Hauser MF, Romero JC, Husmann DA. Electron beam computerized tomography assessment of in vivo single kidney glomerular filtration rate and tubular dynamics during chronic partial unilateral ureteral obstruction in the pig. J Urol 2001;166:2530-2535.
42. Morcos SK, Thomsen HS, Webb JA. Contrast-media-induced nephrotoxicity: a consensus report. Contrast Media Safety Committee, European Society of Urogenital Radiology (ESUR). Eur Radiol 1999;9:1602-1613.

Figure legends

Figure 1. Representative MR images obtained (a) before and (b) after injection of 0.05 mmol kg^{-1} gadoterate dimeglumine and (c) corresponding longitudinal relaxation rate versus time curves in aorta (solid) and renal cortex (dashed). Long arrow in figure 1b indicates aorta, and short arrow, renal cortex.

Figure 2. Renal impulse response (solid) and two fitted gamma variate functions (dashed) corresponding to passage of contrast medium in glomeruli and proximal convoluted tubules. The third peak corresponds to the transit in the distal convoluted tubules and the collecting ducts but is not taken into account in the fit.

Figure 3. Renal cortical longitudinal relaxation rate versus time curve that does not exhibit sequential peaks.

Figure 4. Renal cortical longitudinal relaxation rate versus time curve before deconvolution (solid) and two fitted gamma variate functions (dashed) corresponding to passage of contrast medium in glomeruli and proximal convoluted tubules. Overestimation of peak corresponding to proximal convoluted tubule is clearly apparent.

Figure 5. (a) Correlation between renal perfusion measured by deconvolution method and upslope method. (b) Correlation between GFR measured by deconvolution method and clearance of ^{51}Cr-EDTA.

Figure 6. Relative errors for perfusion (solid), GFR (dashed) (a), and MTT (b) when gaussian noise is added to the curves.

Figures



a)

Figure 1. Representative MR images obtained (a) before and (b) after injection of 0.05 mmol kg^{-1} gadoterate dimeglumine and (c) corresponding longitudinal relaxation rate versus time curves in aorta (solid) and renal cortex (dashed). Long arrow in figure 1b indicates aorta, and short arrow, renal cortex.



b)

Figure 1. Representative MR images obtained (a) before and (b) after injection of 0.05 mmol kg^{-1} gadoterate dimeglumine and (c) corresponding longitudinal relaxation rate versus time curves in aorta (solid) and renal cortex (dashed). Long arrow in figure 1b indicates aorta, and short arrow, renal cortex.

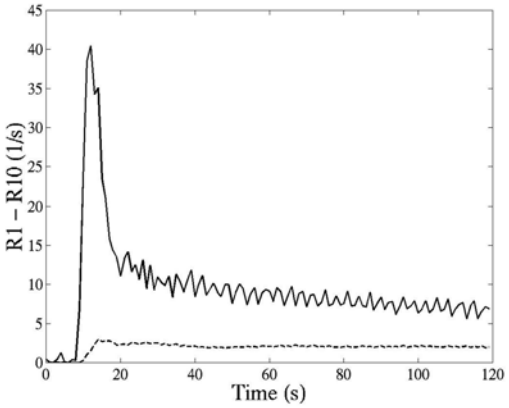

c)

Figure 1. Representative MR images obtained (a) before and (b) after injection of 0.05 mmol kg^{-1} gadoterate dimeglumine and (c) corresponding longitudinal relaxation rate versus time curves in aorta (solid) and renal cortex (dashed). Long arrow in figure 1b indicates aorta, and short arrow, renal cortex.

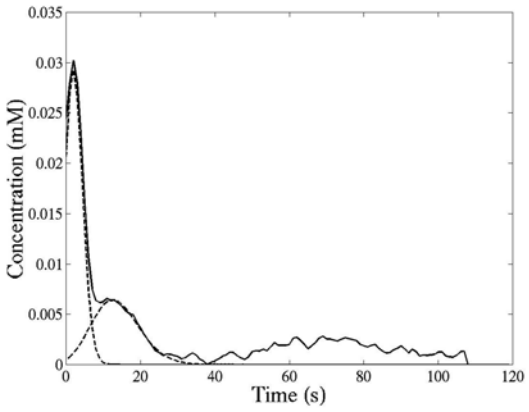

Figure 2. Renal impulse response (solid) and two fitted gamma variate functions (dashed) corresponding to passage of contrast medium in glomeruli and proximal convoluted tubules. The third peak corresponds to the transit in the distal convoluted tubules and the collecting ducts but is not taken into account in the fit.

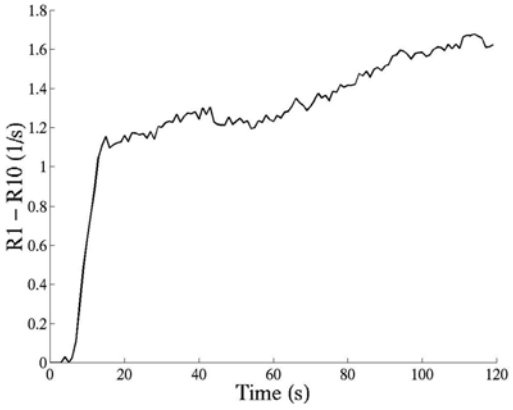

Figure 3. Renal cortical longitudinal relaxation rate versus time curve that does not exhibit sequential peaks.

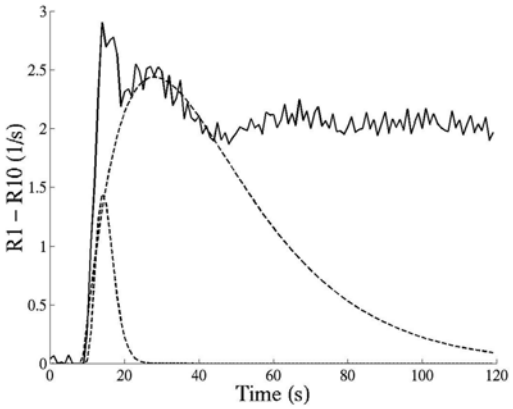

Figure 4. Renal cortical longitudinal relaxation rate versus time curve before deconvolution (solid) and two fitted gamma variate functions (dashed) corresponding to passage of contrast medium in glomeruli and proximal convoluted tubules. Overestimation of peak corresponding to proximal convoluted tubule is clearly apparent.

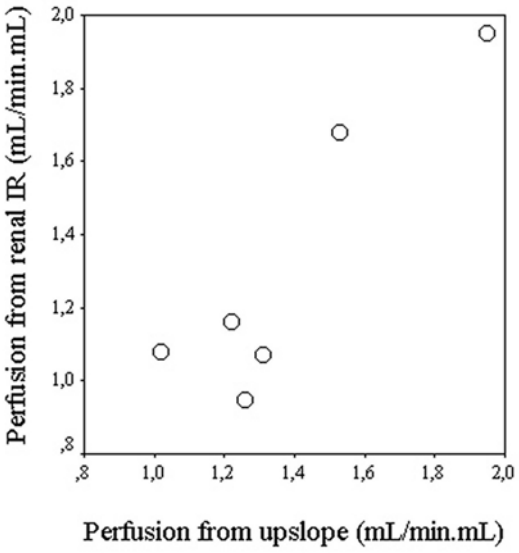

a)

Figure 5. (a) Correlation between renal perfusion measured by deconvolution method and upslope method. (b) Correlation between GFR measured by deconvolution method and clearance of ^{51}Cr-EDTA.

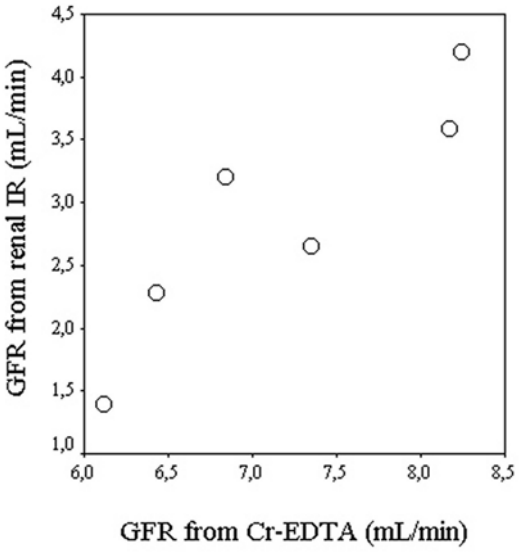

b)

Figure 5. (a) Correlation between renal perfusion measured by deconvolution method and upslope method. (b) Correlation between GFR measured by deconvolution method and clearance of ^{51}Cr-EDTA.

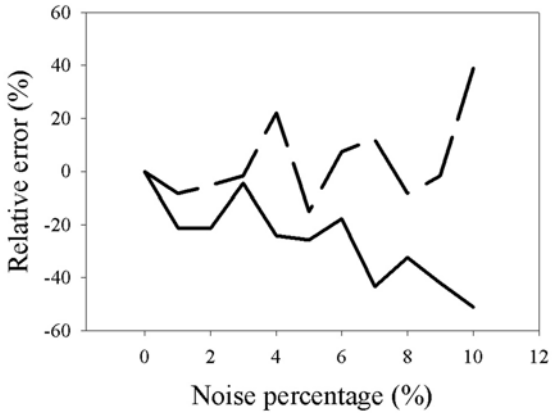

a)

Figure 6. Relative errors for perfusion (solid), GFR (dashed) (a), and MTT (b) when gaussian noise is added to the curves.

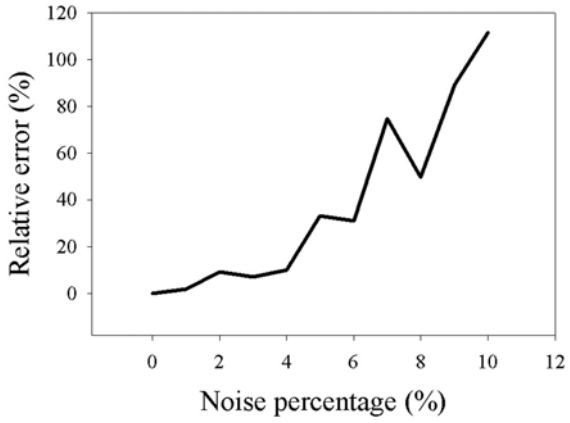

b)

Figure 6. Relative errors for perfusion (a), GFR (a), and MTT (b) when gaussian noise is added to the curves.